

# A Straightforward Approach for the Determination of the Maximum Time Step for the Simulation of Nanometric Metallic Systems

Marcos A. Villarreal,\* Oscar A. Oviedo, and Ezequiel P. M. Leiva

INFIQC, CONICET, Departamento de Matemática y Física, Facultad de Ciencias Químicas, Universidad Nacional de Córdoba, Córdoba, Argentina, X5000HUA

**ABSTRACT:** In the present work, we report on a systematic analysis to determine the maximum time step allowed in molecular dynamics simulations applied to study metal systems of current interest in nanoscience. Using the velocity Verlet integration scheme, we have found that it is possible to use a 20 fs time step for the simulation of gold nanosystems. This is roughly an order of magnitude greater than the usually employed integration step (2 to 5 fs). We also propose a general criterion to select this maximum time step for other metallic nanosystems, even in the case of bimetallic nanosystems.

## ■ INTRODUCTION

Molecular dynamics (MD) simulation has become a well-established tool for the study of physical, chemical, and biochemical systems. This technique allows an efficient exploration of the phase space, from which several important quantities can be calculated. The generation of a trajectory in phase space of any relatively complex system involves the integration of the equations of motion by numerical methods, since analytical solutions exist only for the simplest systems.<sup>1,2</sup> At the heart of any numerical integration method is the selection of an appropriate time step, which determines the quality of the integrated trajectory. This integration time step is mainly bounded by two factors: On the one hand, it has to be small enough to account for the highest frequency of the system. The higher the frequencies, the shorter the time step must be in order to correctly track the dynamics of the system. On the other hand, the time step must be as large as possible in order to accomplish a given simulated time with the least computational effort.

The Störmer–Verlet type of integrators, which includes the Verlet,<sup>3</sup> Leapfrog,<sup>4</sup> velocity Verlet,<sup>5</sup> and Beeman<sup>6</sup> methods, are the most commonly used methods in current MD simulations programs. This is due to their proved stability and simplicity and to the fact that they allow the use of relatively long time steps. It is well established that for the Störmer–Verlet type of integrators, a minimum of 5–10 integration points per period of the highest frequency motion should be performed to achieve reasonable accuracy.<sup>7,8</sup> In molecular systems, the highest frequency motions are the oscillation of the chemical bonds, especially the bonds that involve hydrogen atoms. These motions have a frequency on the order of 3000 cm<sup>-1</sup>; therefore, the maximum time step for a good integration of an unconstrained molecular system must be from 1 to 2 fs.<sup>9</sup> In the case of bulk metallic systems, the highest vibrational frequencies found using inelastic neutron scattering are on the order of 200–400 cm<sup>-1</sup>, depending on the composition of the system.<sup>10–12</sup> When going from bulk materials to nanosystems, the vibrational density of states (DOS) becomes wider. This is explained by a decrease of the vibrational frequencies of the

inner atoms of the material as well as by an increase of the corresponding vibrational frequencies of the surface atoms.<sup>13</sup>

Taking a minimum of five points per period, it should be possible, in principle, to use a time step from 15 to 30 fs, when integrating systems with maximum frequencies between 400 and 200 cm<sup>-1</sup>, respectively. Despite this simple calculation based on the DOS and on the well-known properties of the Störmer–Verlet integrators, the most commonly used time step when simulating metallic nanosystems is from 1 to 2 fs, with occasional use of 5 fs or more. For example, in the study of the melting of metallic nanoparticles (NPs), Sankaranarayanan et al.<sup>14</sup> used 1 fs using the Sutton–Chen potential, Shim et al.<sup>15</sup> used a 4 fs under the modified embedded atom method (MEAM), Liu et al.<sup>16</sup> used 5 fs under the embedded atom method (EAM), Chen et al.<sup>17,18</sup> used a time step of 7 fs under the Gupta potential, and Kietzmann et al.<sup>40</sup> used 10–20 fs and performed quantum MD simulations of 20 ps long. In other MD applications to metallic nanosystems, as the growth of NP or stretching of nanowires, the most popular time is also 2 fs.<sup>19</sup>

Current progress in algorithms, hardware, and software has increased the efficiency of the MD simulations in general, including those of the metallic nanosystems.<sup>20</sup> New algorithms, such as metadynamics,<sup>21</sup> or different types of accelerated dynamics<sup>22</sup> notably increased the exploration of the phase space over regular MD. The GPGPU technology and the corresponding creation or adaptation of the MD software packages for its use<sup>23–25</sup> have almost produced an order of magnitude increase in the simulated time that can be achieved in MD simulations of metallic systems under the EAM potential.<sup>26</sup> The aforementioned potential use of a 15–30 fs instead of the 2–5 fs currently used when simulating metallic nanosystems would signify a further increase of 1 order of magnitude in the computational efficiency of the simulations.

In the present work, we analyze the maximum time step which can be used in MD simulations of metallic nanosystems, by performing standard tests of energy conservation. We also analyze the effect of the time step in the outcome of practical

Received: January 31, 2012

Published: March 28, 2012



applications to systems of current interest in nanoscience. As a result, we elaborate a simple approach for the determination of the maximum time step for the simulation of nanometric metallic systems.

## METHODS

The simulations were performed with the LAMMPS package (June 3, 2011 release), which uses a velocity Verlet integrator.<sup>27</sup> For the simulations of pure metallic systems, the EAM<sup>28,29</sup> parametrization of Sheng et al.<sup>30</sup> was used, while for the bimetallic Ag/Cu system, we employed the EAM parametrization of Williams et al.<sup>31</sup> As a test of the dependency of the results with the potential model employed, the MEAM<sup>32,33</sup> was employed.

For the energy drift test we used a octahedral NP of 201 gold atoms. Prior to the simulations, we performed 10 000 steps of energy minimization and a equilibration to the desired temperature. From this equilibrated structure, 2000 simulations of 1 ps were performed, using a different set of initial velocities in each case. The reported drift in the total energy per degree of freedom (dof) at each time step tested is the average slope of these 2000 energy vs time curves.

For simulations which required constant temperature, the Langevin thermostat<sup>34</sup> was used with a damping factor of 2 ps. We checked the effect of the damping factor in the calculated vibrational DOS and found that only values smaller than 2 ps produced a distortion in the DOS spectrum. The DOS was calculated from the Fourier transform of the velocity autocorrelation function,<sup>41</sup> with velocities saved every 20 fs when possible or every step otherwise. The absolute entropy was calculated with the 2PT theory.<sup>35</sup> In order to obtain converged results in the DOS as well as in the entropy calculation, 50 repetitions of 50 ps each were performed for every time step.

In the simulations of nanowire stretching, we employed a crystal of  $18 \times 7 \times 7$  Å of 80 gold atoms (see Figure 3). The first and last three layers of atoms were kept rigid, resulting in 32 mobile atoms. With this arrangement, the nanowire is able to stretch 6–8 Å before it breaks. The energy vs. extension curve was calculated in a stepwise manner. At every distance, a simulation of 10 ns at 500 K was performed, and the average energy was calculated. After that period, the upper layer of fixed atoms was moved 0.25 Å in the direction of the stretching by the longer axis (see Figure 3). This procedure was repeated 50 times to give a total extension of 12.25 Å in the case of the EAM potential. For simulations with the MEAM potential, the curves were calculated in 18 steps of 0.5 Å. For both potentials, every energy vs. extension curve was repeated, using different initial velocities, 7 (MEAM) and 20 (EAM) times, from which the average and the deviation were calculated and reported in Figures 3 and 4.

In the melting curves, the octahedron of 201 gold atoms was continuously heated from 500 to 1000 K in 200 ns. The potential energy was then averaged in windows of 5 K. Every curve at every time step was repeated 20 times, using different initial velocities, from which the average melting curve and the standard deviation were calculated.

The core–shell NP consisted of a core of 147 copper atoms and a shell of 162 silver atoms. At the simulated temperature of 1000 K, the system was in the liquid state as determined by visual inspection and calculation of the mean square displacement (data not shown). At each time step considered, 200 ns was simulated. The error bars were calculated dividing the

trajectory in five equal portions and treating the results of each portion as independent from each other.

## RESULTS AND DISCUSSION

**Energy Conservation in NVE Simulations.** An important test for a correct setup of a MD simulation is the quality of the energy conservation during a simulation in the NVE ensemble.<sup>8,9</sup> Due to the numerical nature of the integration of the trajectory, any MD simulation in the NVE ensemble will suffer a drift in the total energy. The short-term energy drift was tested by running a set of 2000 1 ps simulations. This large number of simulations is needed to get a reasonable convergence of the results because of the diffusive nature of the energy drift in well integrated systems.<sup>8,36</sup> In Figure 1 we

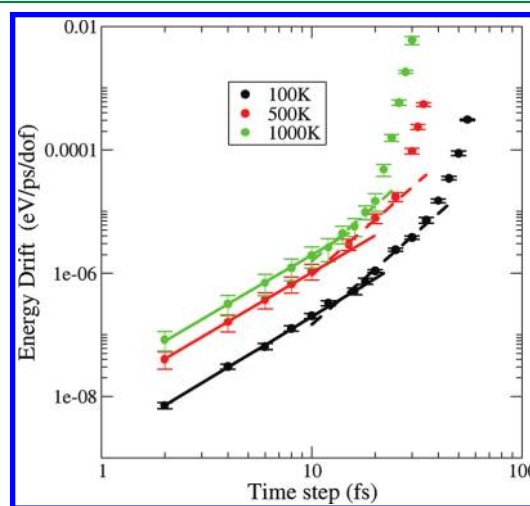


**Figure 1.** Drift in the total energy per degree of freedom for the simulation of a NP in the NVE ensemble as a function of the integration time step, and at different temperatures. Both axes are in a logarithmic scale. The filled dots are the simulation results. The full and dotted lines are fitted to quadratic and cubic functions, respectively.

plot the energy drift as a function of the integration time step for simulations of the NP at three different temperatures. In the range of temperatures explored, the behavior of the NP system goes from that of an almost harmonic solid (100 K) to that of an unharmonic liquid (1000 K). To analyze the order of the energy drift with respect to the time step of the curves in Figure 1, we fitted a quadratic function,  $A \cdot dt^2$ , in the range of 2–6 fs, where  $A$  is a constant and  $dt$  is the integration time step. For the range of 8–12 fs, the fitting function was a cubic one,  $A \cdot dt^3$ . These fitting functions correspond respectively to errors of order 2 and 3, which are the expected ones for the popular Störmer–Verlet type of integration algorithms.<sup>8</sup> It is clear from Figure 1 that the maximum time step for which the error remains within order three decreases with the temperature. At the examined temperatures of 100, 500, and 1000 K, the error remains in order three or less up to 35, 25, and 20 fs, respectively. Beyond these time step lengths, the order of the error increases abruptly indicating the breakdown of the integration algorithm.

**Vibrational Density of States.** In order to assess the effect of the integration time step on the description of the internal motions of a 201 gold atoms NP, we calculated the vibrational DOS. This was achieved by applying the Fourier transform to the velocity autocorrelation function obtained from 50 independent simulations at 500 and 1000 K. At these

temperatures, the NP is in the solid and the liquid states, respectively. Figure 2 shows that when the time step is

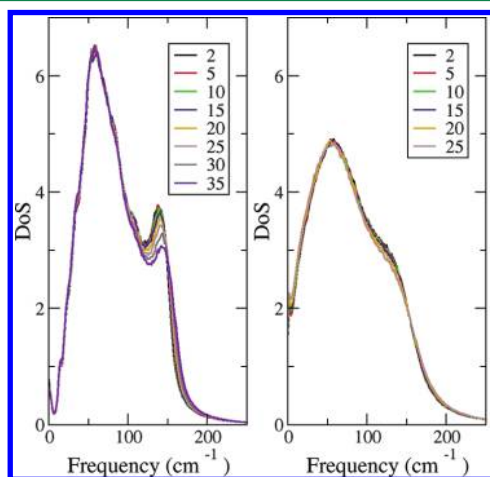


**Figure 2.** Vibrational DOS for the 201 gold NP calculated at 500 and 1000 K (left and right, respectively). The label on each curve indicates (in fs) the time step used.

increased, the DOS spectrum remains almost invariant, conserving the general shape at both temperatures. There is, though, a slight increase in frequency and a reduction of intensity of the peak centered at around  $140\text{ cm}^{-1}$  in the simulations of the solid state at 500 K. This increase in the peak frequency is most evident when the integration step is larger than 20 fs, but it is nevertheless small in all cases, amounting  $3\text{--}4\text{ cm}^{-1}$ . The shift in the peak frequency indicates a problem with the integration of the equations of motion at these frequencies and can be understood from the following analysis: A vibration of  $150\text{ cm}^{-1}$  has a period of 200 fs. Therefore, with a time step of 20 fs there are 10 points for the integration of the motion along this period. For frequencies larger than  $150\text{ cm}^{-1}$ , the integration is made with less than 10 points per period if the time step is larger than 20 fs. Thus, the old rule of thumb that Verlet-type integrators need at least 5–10 points per period to correctly integrate the equations of motions applies in this case.<sup>7,8</sup> As for the liquid state of the NP, at the temperature of 1000 K, the influence of the time step in determining the internal motions of the NP is less evident.

The DOS is a very useful quantity, since it can be used to calculate thermodynamic properties of the system, such as free energy, enthalpy, entropy, etc.<sup>37</sup> These calculations can be accomplished through the use of the Debye theory of crystals,<sup>38</sup> when the system is in the solid state, or by using the 2PT model, which is suitable for the calculation of thermodynamic properties in the solid as well as in the fluid state.<sup>35</sup> In Table 1 we report the absolute entropy calculated with the 2PT formalism for the system at 500 and 1000 K. Within the error of the results, the simulations with the different time steps used here give the same values for the absolute entropy. This indicates that for the sake of calculating thermodynamic properties, the small differences noticed in the DOS spectrum in Figure 2 can be tolerated.

The change in the spectrum observed at high frequencies when the time step is larger than 20 fs is in line with the change found in the order of energy drift observed in Figure 1, which indicated that the integration algorithm was broken. Nevertheless, the simulations made with time steps of 30 and 35 fs at

**Table 1.** Absolute Entropies Per Atom for a 201 Gold Atom NP, as Calculated with the 2PT Formalism<sup>a</sup>

time step (fs)	absolute entropy (J/K/mol)	
	500 K	1000 K
2	64.7 (2.1)	87.6 (1.2)
5	64.3 (2.1)	87.5 (1.3)
10	64.5 (1.9)	87.8 (1.4)
15	64.4 (1.7)	88.2 (1.2)
20	64.4 (2.0)	88.3 (1.1)
25	64.6 (1.9)	89.8 (1.2)
30	64.8 (1.9)	N.D.
35	66.9 (1.9)	N.D.

<sup>a</sup>The quantities in parentheses are two standard deviations. N.D.: Not determined due to instability in the simulations.

500 K and with 25 fs at 1000 K (see Figure 2) show that it is possible to obtain a stable trajectory with a time step longer than that required to remain within the theoretical order in the error of the algorithm. This shows that observing stability in the trajectory does not necessarily imply a well integrated simulation.

**Nanowire Stretching.** As shown in the preceding section, it is possible to obtain a stable trajectory even using a time step longer than the limit of the theoretical stability of the algorithm. Therefore, in this and the next two sections we analyze the effect of an increasingly longer time step in simulations of different systems with relevance in nanoscience to further check the maximum allowed time step. We compare these results with simulations performed with 2 fs time step, which will be considered as the correct or expected outcome of the model. Thus, any deviation from the results obtained with 2 fs will be taken as indicative of problems due to the integration. In Figure 3 we plot the difference in potential energy of a gold nanowire as a function of the distance between its ends. The inset in Figure 3 shows some typical configurations along the stretching path. This kind of stretching simulation is typically used in the study of the mechanical deformation of nanowires using atomistic simulations.<sup>19,39</sup> In Figure 3 the energy vs. elongation

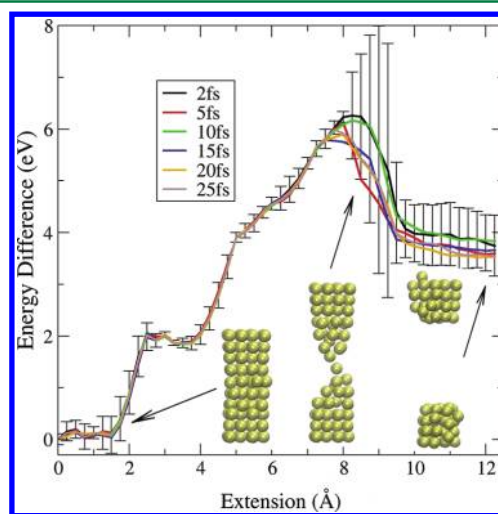


**Figure 3.** Energy vs extension curves for the stretching of an 80 gold atom nanowire using the EAM potential. The label on each curve indicates (in fs) the time step used. Representative structures along the reaction coordinate are shown in the inset. For simplicity, only the error bars of the simulation with 2 fs are shown.



curve made with the EAM potential shows that the nanowire can extend, on average, up to 8 Å from the initial configuration before it breaks. The energy difference between the relaxed nanowire and the breaking point is, on average, 6 eV for the present configuration. After the rupture is produced, a large variety of structures are formed, and therefore the dispersion in the energy is bigger than before it. For the present work, the important result is that all the time steps explored (up to 25 fs) produce the same energy vs. extension profiles within the error of the result obtained from the 2 fs simulation. Simulations with time step longer than 25 fs were not always stable. In Figure 4,

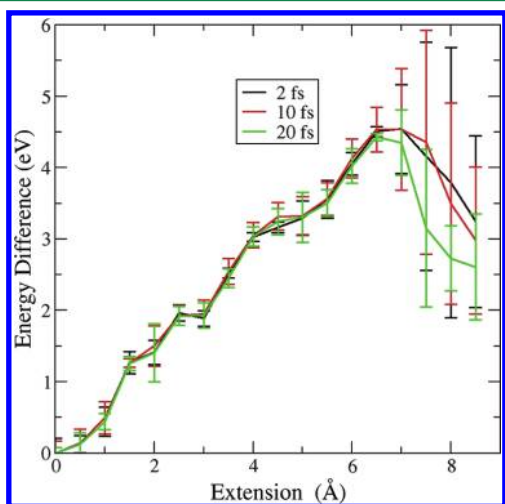


**Figure 4.** Energy vs extension curves for the stretching of an 80 atoms gold nanowire using the MEAM potential. The label on each curve indicates the time step used to integrate the equations of motion. The error bars correspond to two standard deviations from seven repetitions.

the same experiment is conducted with the MEAM potential. In this case, the nanowire breaks with a lower energy difference (4.5 eV) and at a lower extension (6.5 Å), but again the results from simulations carried out with time steps up to 20 fs are indistinguishable. This would indicate that the limit of 20–25 fs is intrinsic to the nanosystems made up of gold atoms and not to the model potential.

**NP Melting.** The melting of a octahedral NP of 201 gold atoms using the EAM potential was studied as a function of the integration time step. The energy vs. temperature curves shown in Figure 5 are the average of 20 simulation runs, in which each realization started with a different set of velocities. The melting of the NP was determined to start around 700 K. At temperatures near melting, the error in the energy increases notably. This is due to the fact that the solid to liquid transition occurs at slightly different temperatures in the different repetitions, as a consequence of the small size of the system.

The melting curves shown in Figure 5 are indistinguishable from each other within the error bars when using time steps from 2 to 20 fs. Only the curve made with 25 fs is clearly different from the rest, again indicating that obtaining a stable trajectory does not imply obtaining the correct result from the simulation. Simulations with time step longer than 25 fs were not always stable.

**Bimetallic NP in the Liquid State.** As a further test for a system with relevance to nanoscience, we studied the equilibrium properties of a Cu–Ag core–shell NP at 1000 K. At this temperature, the NP is in the liquid state. The

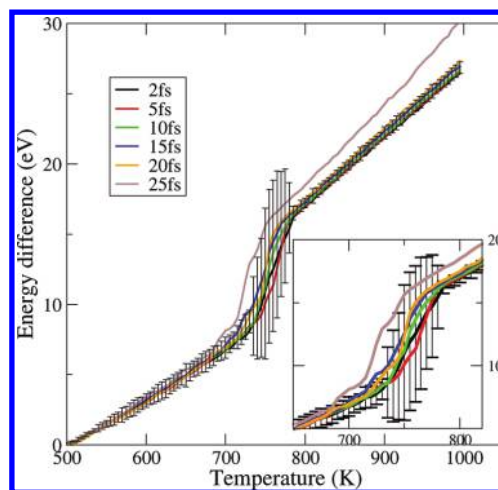


**Figure 5.** Melting curve for a 201 gold atom NP. The inset shows the transition region in detail. For simplicity, only the error bars of the simulation with 2 fs are shown. The label on each curve indicates (in fs) the time step used.

distribution of the Cu and Ag as a function of the distance from the center of mass (CoM) of the particle is shown in Figure 6.

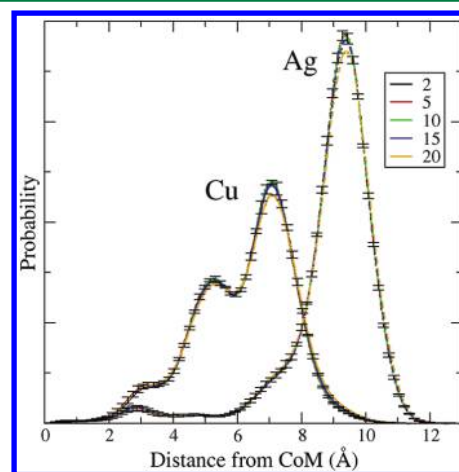


**Figure 6.** Distribution of Cu and Ag from the center of mass in a core–shell NP. For simplicity, only the error bars of the simulation with 2 fs are shown. The label on each curve indicates (in fs) the time step used.

From this figure it is clear that the Cu is mostly forming the core. Ag prefers the outer part of the NP, thus forming the shell, although a small spike in the distribution curve of Ag is evident in the center of the NP. Within the error bars, the curves made with different time steps are equal, except for the simulations made with 20 fs. In this case, the value of the maximum probability is lower than for the rest of the simulations. As these distributions are normalized, the curves for the 20 fs time step must be wider than the rest in order to compensate for lower probability at the maximum. This is not evident in Figure 6, and hence we computed the radius of gyration of the NP to spot out this effect. In Figure 7, it is clear that the simulations with 20 fs result in a NP which is somewhat bigger than the reference made with 2 fs time step. From the above results, the maximum time step which produces results in accordance to the 2 fs simulations is around 15 fs.

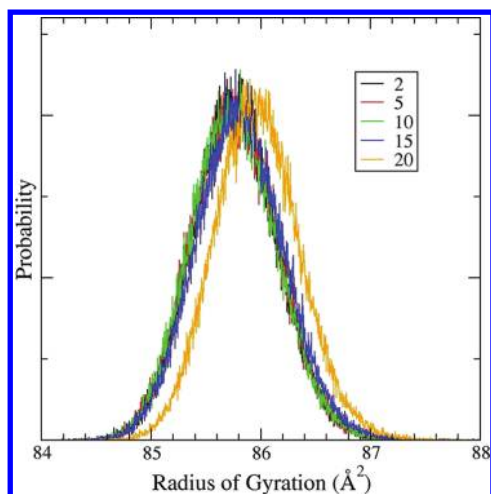


**Figure 7.** Distribution of radius of gyration in the Cu–Ag core–shell NP. The label on each curve indicates (in fs) the time step used.

**Extension to Other Metals.** In this section we elaborate a heuristic methodology to determine the maximum integration time step allowed for different metallic nanosystems. First, we recognize that, based on the results for the pure gold systems tested (i.e., the DOS, the stretching of a nanowire, and the melting of the NP), the maximum time step can be established to be 20 fs. This is because 20 fs is the point at which the energy drift remains at or below an order of three at 1000 K (Figure 1). As the DOS is easier to calculate than the energy drift curve, we elaborate an heuristic criterion based on the DOS instead of the energy drift. If we integrate the DOS curves of Figure 2, which correspond to the gold NP, we find that with a time step of 20 fs, 99% of the different frequencies are integrated with 7 or more points per period. In order to test if this observation holds for different metals, we calculated the DOS and the energy drift, both at 1000 K, using the same NP as before. Figure 8 shows the resulting DOSs. It can be observed that for the metals tested, the curves are ordered according to the atomic weight. Pb presents the lowest vibration frequencies, while the lightest metal considered, Al, presents the highest frequencies. The time step with which 99%

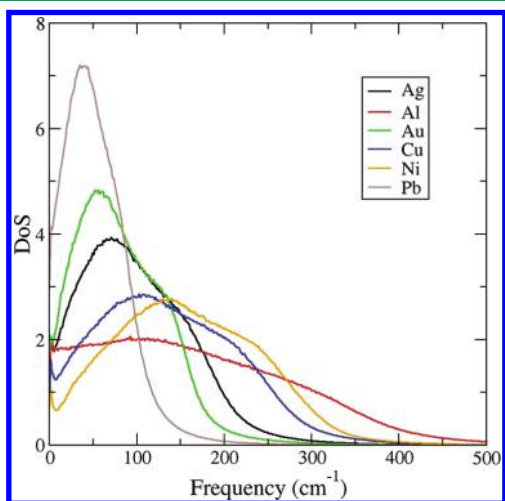


**Figure 8.** Vibrational DOSs for a 201 atom NP of different metals. The simulations were made with a 2 fs time step and at a temperature of 1000 K.

of the frequencies are integrated with at least 7 points per period is shown in Table 2. In this table we also present the

**Table 2.** Maximum Time Steps Suggested for Simulating Metallic Nanosystems<sup>a</sup>

metal	tm1	tm2
Ag	16	16
Al	10	12
Au	19	20
Cu	14	15
Ni	13	14
Pb	26	28

<sup>a</sup>tm1 was determined using the heuristic criterion that 99% of the frequencies are integrated with at least 7 points per period, and tm2 was determined by setting the condition that the order of the energy drift must remain below three.

maximum time step for which the integration is stable, i.e., the order of the energy drift (Figure 9) remains below or equal to

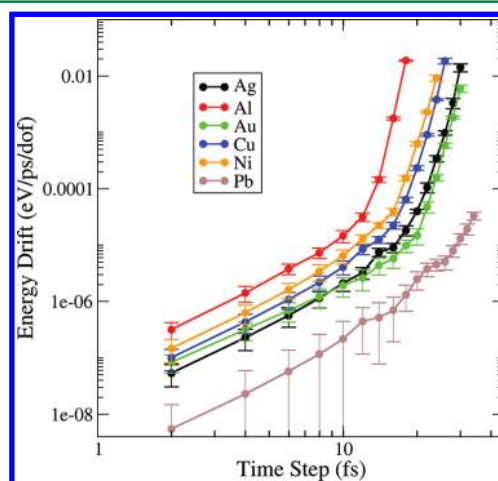


**Figure 9.** Drift in the total energy per degree of freedom as a function of the integration time step for different metallic NPs at 1000 K. The axes are in a logarithmic scale. The filled dots are the result of the simulations, and the lines are a guide to the eye.

three. The maximum time steps determined by both methods are in agreement, and therefore the criterion of the 99% is a good indicator of the breakdown of the integration algorithm.

From Table 2 it can be inferred that the maximum time steps for a system made up of Ag or Cu are 16 and 15 fs, respectively. Thus, for systems containing both metals, it is possible to assume that the maximum time step allowed should be around 15 fs. According to the results in the preceding section (Figures 6 and 7), the simulations of the Cu–Ag core–shell NP produce the same results until a time step of 15 fs, in line with the values of Table 2 and supporting the heuristic proposed.

**CPU Efficiency.** The CPU efficiency of a simulation, i.e., the number of ns simulated per CPU hour, does not necessarily increase linearly with the length of the time step. This is due to the overhead of neighbor list generation, printing frequency, coordinate communications between processor (if the simulation is run in parallel), etc. Through the simulations performed in the present work, the observed speed-up using 4, 10, and 20 fs, with respect to the simulations using 2 fs, was 2, 4.8, and 9, respectively. In practice this speed-up means that in a given CPU time, the phase space of the system is better

explored, which in turn results in lower statistical errors in the calculated properties of the system. Recently, Rao and Spichty<sup>42</sup> showed that even using a long integration time step which slightly modifies the free energy surface of the system (a fact that is not observed for the systems studied in this work), the enhanced exploration of the phase space is beneficial in terms of the lower statistical errors on the calculated observables.

## CONCLUSIONS

In the present work we have explored the effect that the use of relatively large time steps produces on the results of MD simulations performed for different nanometric metallic systems. The selected integration algorithm was the velocity Verlet one, which has been widely employed in the literature. It was found that time steps up to 1 order of magnitude larger than those usually employed deliver results for different properties that are within the error bars of the latter. A general criterion is proposed to select this maximum time step for other systems: 99% of the frequencies found in the phonon spectrum of the nanosystem must be integrated with at least 7 points per period.

## AUTHOR INFORMATION

### Corresponding Author

\*E-mail: arloa@fcq.unc.edu.ar

### Notes

The authors declare no competing financial interest.

## ACKNOWLEDGMENTS

We acknowledge CONICET PIP: 112-200801-000983, Secyt (Universidad Nacional de Córdoba), Program BID (PICT 2006 Nr 946 and PICT 2010 Nr 123), and PME: 2006-01581 for financial support.

## REFERENCES

- (1) Allen, M. P.; Tildesley, D. J. In *Computer Simulation of Liquids*; Clarendon Press: Oxford, U.K., 1991.
- (2) Frenkel, D.; Smit, B. In *Understanding Molecular Simulation: from Algorithms to Applications*; Academic Press: San Diego, CA, 2002.
- (3) Verlet, L. *Phys. Rev.* **1969**, *159*, 98–103.
- (4) Hockney, R. W.; Eastwood, J. W. In *Computer Simulation Using Particles*; McGraw-Hill: New York, 1981.
- (5) Swope, W. C.; Andersen, H. C.; Berens, P. H.; Wilson, K. R. *J. Chem. Phys.* **1982**, *76*, 637–649.
- (6) Beeman, D. J. *Comput. Phys.* **1976**, *20*, 130–139.
- (7) Levitt, M. J. *Mol. Biol.* **1983**, *168*, 595–620.
- (8) Mazur, A. K. *J. Comput. Phys.* **1997**, *136*, 354–365.
- (9) Mazur, A. K. *J. Phys. Chem. B* **1998**, *102*, 473–479.
- (10) Lynn, J. W.; Smith, H. G.; Nicklow, R. M. *Phys. Rev. B* **1973**, *8*, 3493–3499.
- (11) Nilsson, G.; Rolandson, S. *Phys. Rev. B* **1973**, *7*, 2993–2400.
- (12) Birgeneau, R. J.; Cordes, J.; Dolling, G.; Woods, A. D. B. *Phys. Rev.* **1964**, *136*, A1359–A1365.
- (13) Kara, A.; Rahman, T. S. *Phys. Rev. Lett.* **1998**, *81*, 1453–1456.
- (14) Sankaranarayanan, S. K. R. S.; Bhethanabotla, V. R.; Joseph, B. *Phys. Rev. B* **2005**, *71*, 195415/1–195415/15.
- (15) Shim, J.-H.; Lee, B.-J.; Cho, Y. W. *Surf. Sci.* **2002**, *512*, 262–268.
- (16) Liu, H. B.; Pal, U.; Perez, R.; Ascencio, J. A. *J. Phys. Chem. B* **2006**, *110*, 5191–5195.
- (17) Chen, F.; Curley, B. C.; Rossi, G.; Johnston, R. L. *J. Phys. Chem. C* **2007**, *111*, 9157–9165.
- (18) Chen, F.; Johnston, R. L. *ACS Nano* **2008**, *2*, 165–175.
- (19) Pu, Q.; Leng, Y.; Tsetseris, L.; Pantelides, S. T.; Cummings, P. T. *J. Chem. Phys.* **2007**, *126*, 144707–144716.
- (20) Nielaba, P.; Mareschal, M.; Ciccotti, G. In *Bridging Time Scales: Molecular Simulations for the Next Decade*; Springer-Verlag: Berlin, Germany, 2002.
- (21) Laio, A.; Parrinello, M. *Proc. Natl. Acad. Sci. U.S.A.* **2002**, *99*, 12562–12566.
- (22) Perez, D.; Uberuaga, B. P.; Shim, Y.; Amar, J. G.; Voter, A. F. In *Annual Reports in Computational Chemistry*; Elsevier: Amsterdam, The Netherlands, 2009; Vol 5, Chapter 4.
- (23) Harvey, M. J.; Giupponi, G.; De Fabritiis, G. *J. Chem. Theory Comput.* **2009**, *5*, 1632–1639.
- (24) Brown, W. M.; Wang, P.; Plimpton, S. J.; Tharrington, A. N. *Comput. Phys. Commun.* **2011**, *182*, 898–911.
- (25) Anderson, J. A.; Lorenz, C. D.; Travesset, A. *J. Comput. Phys.* **2008**, *227*, 5342–5359.
- (26) Morozov, I. V.; Kazennova, A. M.; Bystryia, R. G.; Normana, G. E.; Pisareva, V. V.; Stegailova, V. V. *Comp. Phys. Comp.* **2011**, *182*, 1974–1978.
- (27) Plimpton, S. J. *Comp. Phys.* **1995**, *117*, 1–19.
- (28) Daw, M. S.; Baskes, M. I. *Phys. Rev. Lett.* **1983**, *50*, 1285–1288.
- (29) Daw, M. S.; Baskes, M. I. *Phys. Rev. B* **1984**, *29*, 6443–6453.
- (30) Sheng, H. W.; Kramer, M. J.; Cadieu, A.; Fujita, T.; Chen, M. W. *Phys. Rev. B* **2011**, *83*, 134118/1–134118/20.
- (31) Williams, P. L.; Mishin, Y.; Hamilton, J. C. *Model. Simul. Mater. Sci. Eng.* **2006**, *14*, 817–833.
- (32) Baskes, M. I. *Phys. Rev. B* **1992**, *46*, 2727–2742.
- (33) Valone, S. M.; Baskes, M. I.; Martin, R. L. *Phys. Rev. B* **2006**, *73*, 214209/1–214209/11.
- (34) Schneider, T.; Stoll, E. *Phys. Rev. B* **1978**, *17*, 1302–1322.
- (35) Lin, S.-T.; Blanco, M.; Goddard, W. A. *J. Chem. Phys.* **2003**, *119*, 11792–11805.
- (36) Feenstra, K. A.; Hess, B.; Berendsen, H. J. C. *J. Comput. Chem.* **1999**, *20*, 786–798.
- (37) Chui, Y. H.; Grochola, G.; Snook, I. K.; Russo, S. P. *Phys. Rev. B* **2007**, *75*, 033404/1–033404/4.
- (38) McQuarrie, A. A. *Statistical Mechanics*; Harper & Row: New York, 1976.
- (39) Kang, J.; Hwang, H. *Nanotechnology* **2001**, *12*, 295–300.
- (40) Kietzmann, A.; Redmer, R.; Hensel, F.; Desjarlais, M. P.; Mattsson, T. R. *J. Phys.: Condens. Matter.* **2006**, *18*, 5597–5605.
- (41) Haile, J. M. *Molecular Dynamics Simulation*; Wiley: New York, 1992; p 277.
- (42) Rao, F.; Spichty, M. *J. Comput. Chem.* **2012**, *33*, 475–483.